Mechanical Systems and Signal Processing 117 (2019) 1–15

Contents lists available at ScienceDirect

Mechanical Systems and Signal Processing

journal homepage: www.elsevier.com/locate/ymssp

Vibration-based structural health monitoring under changing environmental conditions using Kalman filtering

Kalil Erazo [a,b], Debarshi Sen [a], Satish Nagarajaiah [a,c,*], Limin Sun [d]

[a] Department of Civil and Environmental Engineering, Rice University, Houston, TX 77005, USA
[b] Área de Ingenierías, Instituto Tecnológico de Santo Domingo, Santo Domingo 10602, Dominican Republic
[c] Department of Mechanical Engineering, Rice University, Houston, TX 77005, USA
[d] Department of Civil Engineering, Tongji University, China

ARTICLE INFO

Article history:
Received 10 August 2017
Received in revised form 15 July 2018
Accepted 21 July 2018
Available online 2 August 2018

Keywords:
Structural health monitoring
Damage identification
Kalman filtering
Environmental effects

ABSTRACT

A Kalman filtering based framework for structural damage assessment under changing environmental conditions is presented. The approach is based on the well-known property that the filtering residual is a realization of a white stochastic process when the filter is operating under optimal conditions. To decouple structural damage and environmental effects two additional properties of the filtering residual are employed: i) under global changes in the structure caused by environmental variations the residual remains a white process, and thus its spectral density is approximately constant; ii) local changes caused by structural damage induce peaks in the residual spectral density at the affected vibration frequencies, and thus the residual is a colored process. A Bayesian whiteness test is employed to discriminate between the two situations under finite length data conditions (damage detection), while a normalized damage measure based on the spectral moments of the residual spectral density is proposed as a quantitative damage-sensitive feature (damage quantification). The proposed approach is numerically verified in a continuous beam model of a bridge under different operating conditions, including a robustness assessment for non-uniform temperature fields. It is shown that the approach has the capability to decouple physical changes caused by structural damage and varying environmental conditions, providing robust damage measures for structural health monitoring applications.

1. Introduction

Structural health monitoring (SHM) is the process of using information obtained from an array of sensors deployed on a structural or mechanical system to infer its state of structural integrity (damage diagnosis) and to estimate its remaining useful life (damage prognosis) [1–3]. The premise of most structural damage diagnosis methods is that physical changes in a system are reflected in its dynamic properties (mainly vibration frequencies, mode shapes and damping ratios) and/or in response-based damage measures [4–6]. A limitation constraining the use of SHM approaches in applications is that structural damage is not the only cause of variations in the dynamic characteristics of structural and mechanical systems.

* Corresponding author at: Department of Civil and Environmental Engineering, Rice University, Houston, TX 77005, USA.
E-mail addresses: Kalil.Erazo@intec.edu.do (K. Erazo), Debarshi.Sen@rice.edu (D. Sen), Satish.Nagarajaiah@rice.edu (S. Nagarajaiah), lmsun@tongji.edu.cn (L. Sun).

https://doi.org/10.1016/j.ymssp.2018.07.041
0888-3270/

In particular it has been shown that environmental effects have an important influence in the dynamic properties of structures that cannot be neglected by SHM methods [7–10]. In fact, it has been shown that variations induced by environmental effects are such that they can completely mask structural damage in applications [11–14]. This poses an obstacle for damage detection techniques since their reliability becomes questionable due to the increase in the probability of false-positive and false-negative damage estimates. Among the various environmental effects that influence structural behavior, variations in the temperature field have shown to be the one that tends to dominate in SHM applications [9]. Under these conditions SHM methods need to be able to decouple structural damage from variations in the temperature field. In other words, if the measured response and/or the estimated damage sensitive features of a structure at a given time show departure from a reference healthy state, how can we assess if the change is caused by normal fluctuations in the environment or structural damage.

Although both structural damage and fluctuations in the temperature field affect the dynamic characteristics of structures, the effects show systematic patterns that can be exploited to decouple them using vibration response measurements. In particular environmental effects tend to induce global changes that affect all the vibration properties in a somewhat uniform fashion, while structural damage tends to affect the structure locally, resulting in some vibration modes being affected significantly more than others [15]. For example, in many practical applications the overall shape of the vibration modes remain almost unaffected by variations in the temperature field, since the field is typically smooth and continuous in space and time. On the other hand, structural damage tends to induce local variations in the curvature of the mode shapes that are more pronounced in the damaged regions [16].

The difference in the sensitivity of the dynamic properties of structures to damage and temperature variations implies that their effect in response measurements can be used to solve the inverse problem of tracking back the source of the change. For this purpose different approaches have shown to be effective under different operating conditions, but mainly for homogeneous systems [17,18]. In Ref. [9] Sohn et al. developed and validated a static linear regression model using data from the Alamosa Canyon Bridge. The confidence intervals obtained were used to discriminate changes caused by environmental effects and structural damage. Regression models were further extended to account for dynamic effects using an auto-regressive exogenous ARX model [19,20]; this model takes into account thermal dynamics, i.e., the dependence of the current dynamic properties in the past time-history of the temperature field. In Ref. [19] Peeters and De Roeck validated the model using data from the Z24 bridge in Switzerland, while in Ref. [20] Moaveni and Behmanesh validated the model using data from a footbridge under different operating conditions. Another approach was proposed in Ref. [21] by Fritzen et al., where a residual is computed by comparing the response of the potentially damaged structure with a reference undamaged state; for this purpose the reference response is stored in the form of singular vectors at different temperatures. When measurements from the potentially damaged structure are gathered at a given temperature, the residual is computed by projecting to the stored reference data. This approach assumes that the subspaces spanned by the reference and damaged data are orthogonal. The use of modal filters to decouple structural damage and environmental effects was proposed by Deraemaeker et al. in Ref. [22]; the proposed approach is based on modal filters calibrated such that a peak appears in the frequency domain output of the filter in the presence of damage. In Ref. [17] Yan et al. proposed an output-only linear approach based on principal component analysis (PCA) to discriminate environmental changes from structural damage. Damage is assessed by novelty detection using the Euclidean norm or a Mahalanobis distance of residual errors; the approach assumes that the variations of temperature and damage are orthogonal. The PCA approach was further extended to account for nonlinearities using piecewise linear approximations and employing PCA for the different linear regions (local PCA) [23]. More recently a residual-based approach based on kernel PCA was proposed to account for temperature-induced nonlinearities using a non-parametric model [24]. The approach was validated using data from the Z24 bridge in Switzerland.

In this paper a statistical approach to decouple structural damage and temperature variations is presented. The approach relies on a Kalman filter model to estimate the residual error (difference between measurement and response estimate), and a Bayesian whiteness test as a damage-sensitive feature. It is well-known that when the Kalman filter operates under optimal conditions the residual is a white process, and thus the residual power spectral density (PSD) is constant [25]. The following two additional properties of the residual PSD are employed herein to decouple temperature and damage effects: i) under global changes caused by environmental variations the residual spectral density remains approximately constant; ii) local changes caused by damage induce peaks in the residual PSD, and thus the residual is a colored stochastic process. The previous Kalman filtering residual properties imply that structural damage induces a correlation in the residual process, while the residual process remains a white process under variations in the temperature field. The properties will be used to develop a framework to decouple structural damage from variations in the temperature field. The average air temperature at the structure location is assumed to be known.

To assess if a realization of the residual process qualifies (in a statistical sense) as a white process under finite length data conditions a Bayesian whiteness test is proposed, while to quantify structural damage a normalized damage index based on the spectral moments of the residual PSD is proposed. The paper is organized as follows: first, the fundamentals of the Kalman filter are briefly revised, followed by an analysis of the correlations induced in the filter residual by both structural damage and temperature variations. Then, the proposed Bayesian whiteness test is introduced for damage detection, followed by a discussion of the proposed normalized damage index introduced for damage quantification. Finally, a numerical results section illustrates the application of the framework in a continuous steel beam model of a bridge subjected to uniform and non-uniform temperature fields.

2. Stochastic model and Kalman filtering

Structural systems under changing environmental conditions can be modeled during short time intervals (in the order of minutes) as linear time-invariant systems with the state-space representation

$$\dot{x}(t) = \mathbf{A}x(t) + \mathbf{B}w(t) \tag{1}$$

where $x(t) \in \mathbb{R}^n$ is the state at time t, $\mathbf{A} \in \mathbb{R}^{n\times n}$ is the state transition matrix, and $\mathbf{B} \in \mathbb{R}^{n\times r}$ is the input to state matrix. The stochastic process w is formally a white process with spectral density matrix $\mathbf{Q} \in \mathbb{R}^{r\times r}$, used to model ambient excitations and/or operating conditions (traffic, wind, waves, among others); the process w can be filtered to achieve a target spectral density for the input. The output (measurement) vector $y(t) \in \mathbb{R}^m$ is given by

$$y(t) = \mathbf{C}x(t) + \mathbf{D}w(t) + \eta(t) = \mathbf{C}x(t) + v(t) \tag{2}$$

where $\mathbf{C} \in \mathbb{R}^{m\times n}$ is the state to output matrix, $\mathbf{D} \in \mathbb{R}^{m\times r}$ is the direct transmission matrix and m is the number of measurements. The stochastic process η is formally a white process with spectral density $\mathbf{N}$, used to model measurement noise, and $v = \mathbf{D}w + \eta$ is a white process with spectral density $\mathbf{R}$. The processes w and η are assumed to be zero mean and statistically independent.

When the matrices $\{\mathbf{A}, \mathbf{B}, \mathbf{C}, \mathbf{D}, \mathbf{Q}, \mathbf{N}\}$ are known, an optimal (in some predefined sense) estimate of the state can be computed. The optimal estimate of the state in the sense of minimizing the mean-square error is given by the Kalman filter (KF) [26]. If the system is observable and controllable the filtering process reaches a unique steady-state solution

$$\dot{\hat{x}}(t) = \mathbf{A}\hat{x}(t) + \mathbf{K}e(t) = (\mathbf{A} - \mathbf{KC})\hat{x}(t) + \mathbf{K}y(t) \tag{3}$$

where $\hat{x}$ is the estimate of x, the matrix $\mathbf{K} \in \mathbb{R}^{n\times m}$ is the Kalman gain, and $e(t)$ is the measurement residual (also known as the innovations), given by

$$e(t) = y(t) - \hat{y}(t) = y(t) - \mathbf{C}\hat{x}(t) \tag{4}$$

or

$$y(t) = \mathbf{C}\hat{x}(t) + e(t) \tag{5}$$

The steady-state Kalman gain $\mathbf{K}$ is given by

$$\mathbf{K} = \mathbf{P}\mathbf{C}^T\mathbf{R}^{-1} \tag{6}$$

where $\mathbf{P} = \mathbb{E}\left[(\hat{x} - x)(\hat{x} - x)^T\right]$ is the state error covariance matrix, computed as the solution of the following Ricatti equation [27]

$$\mathbf{A}\mathbf{P} + \mathbf{P}\mathbf{A}^T + \mathbf{B}\mathbf{Q}\mathbf{B}^T - \mathbf{P}\mathbf{C}^T\mathbf{R}^{-1}\mathbf{C}\mathbf{P} = 0 \tag{7}$$

From Eqs. (3) and (5) the Kalman filter can be interpreted as an equivalent open-loop dynamic system with the residual as input, the measurement as output, and the Kalman state estimate as the state. A data-driven approach can be employed to obtain a realization $\{\mathbf{A}_d, \mathbf{C}_d, \mathbf{K}_d\}$ of the discretized system matrices, and an estimate of the Kalman states from limited response measurements [28]. It is worth to point out that although the system realization is in an arbitrary coordinate system, the product $\mathbf{C}_d\hat{x}$ is in physical coordinates as seen from Eq. (5). This is of prime importance for the practical application of the residual-based approach presented later in this paper.

The stochastic model discussed above is a linear time-invariant model to be used for different temperature ranges in time intervals in the order of minutes. Thus, the identified matrices can be written as a function of temperature T as $\{\mathbf{A}_d(T), \mathbf{C}_d(T), \mathbf{K}_d(T)\}$; the realization is computed for the baseline (healthy) system for the range $T \in (T_0, T_f)$ under operating conditions. When data from the potentially damaged structure at a given interrogation temperature T_I is available, the correlations of the residual are used to assess the state of structural integrity using statistics-based damage measures as discussed in a further section of the paper.

The damage sensitive features employed in this paper are based on a well-known property of the residual, namely, that when the Kalman filter operates under optimal conditions the stochastic process e is a white process [25]. Correlations in the residuals are introduced by structural damage, while the residual remains unaffected by temperature variations, as discussed in the following section.

2.1. Residual correlations induced by damage and temperature variations

To develop an effective and robust damage measure it is useful to study how correlations are induced in the residuals when the Kalman filter is operating under sub-optimal conditions. Residual correlations have shown to be an effective damage-sensitive feature under ideal modeling conditions and in the presence of errors in the description of the forcing input statistics [29,30]. In fact, residuals and output measurements are statistically equivalent (in the sense that they contain

the same statistical information) as long as only linear transformations are involved [31]. The use of residual correlations as a damage-sensitive feature is extended herein to decouple structural damage from variations in the temperature field.

We will first examine the residual correlations induced by structural damage and temperature effects, modeled in a parametric fashion as a change in the system matrix from $\mathbf{A}$ to $\bar{\mathbf{A}} = \mathbf{A} + \Delta A$. The main difference between the two sources is that temperature effects tend to affect almost all the vibration frequencies in a somewhat uniform fashion (global changes), causing a shift of most of the poles with the modes of vibration remaining almost unaffected (up to a scaling factor). On the other hand, structural damage tends to induce local changes that affect a small subset of the vibration frequencies in a more pronounced manner. Moreover, the modes of vibration are affected locally, with curvature variations that are usually larger in the damaged region [16].

2.2. Time domain analysis

Defining the state estimation error as $\tilde{x}(t) = \hat{x}(t) - x(t)$, the residual in Eq. (4) is given by

$$e(t) = \mathbf{C}(x(t) - \hat{x}(t)) + v(t) = -\mathbf{C}\tilde{x}(t) + v(t) \tag{8}$$

The residual correlation matrix is (for $t_2 > t_1$)

$$\mathcal{R}_{ee}(t_2, t_1) = \mathbb{E}\left[e(t_2)e^T(t_1)\right] = \mathbf{C}\mathbb{E}\left[\tilde{x}(t_2)\tilde{x}^T(t_1)\right]\mathbf{C}^T - \mathbf{C}\mathbb{E}\left[\tilde{x}(t_2)v^T(t_1)\right] + \mathbf{R}\delta(t_2 - t_1) \tag{9}$$

where δ is the Dirac delta function, $\mathbb{E}[\cdot]$ denotes the expectation operator, and the fact that $v(t_2)$ is orthogonal to $\tilde{x}^T(t_1)$ was used. Using Eq. (1) (with $\bar{\mathbf{A}}$ replacing $\mathbf{A}$) and Eq. (3), the estimation error is governed by

$$\dot{\tilde{x}}(t) = (\mathbf{A} - \mathbf{KC})\tilde{x}(t) - \Delta A x(t) + \mathbf{K}v(t) - \mathbf{B}w(t) \tag{10}$$

As can be seen, the estimation error is coupled with the state. To handle the coupling the equations can be written in the augmented form

$$\begin{bmatrix} \dot{x}(t) \\ \dot{\tilde{x}}(t) \end{bmatrix} = \begin{bmatrix} \bar{\mathbf{A}} & \mathbf{0} \\ -\Delta A & \mathbf{A} - \mathbf{KC} \end{bmatrix} \begin{bmatrix} x(t) \\ \tilde{x}(t) \end{bmatrix} + \begin{bmatrix} \mathbf{B} \\ -\mathbf{B} \end{bmatrix} w(t) + \begin{bmatrix} \mathbf{0} \\ \mathbf{K} \end{bmatrix} v(t) \tag{11}$$

where $\mathbf{0}$ is a zero matrix of appropriate dimensions. Defining

$$\mathbf{H} = \begin{bmatrix} \bar{\mathbf{A}} & \mathbf{0} \\ -\Delta A & \mathbf{A} - \mathbf{KC} \end{bmatrix} \quad \mathbf{T} = \begin{bmatrix} \mathbf{B} \\ -\mathbf{B} \end{bmatrix} \quad \mathbf{U} = \begin{bmatrix} \mathbf{0} \\ \mathbf{K} \end{bmatrix} \tag{12}$$

Eq. (11) is written more compactly as

$$\dot{z}(t) = \mathbf{H}z(t) + \mathbf{T}w(t) + \mathbf{U}v(t) \tag{13}$$

where $z = [x^T \ \tilde{x}^T]^T$. The closed-form solution of Eq. (13) is given by

$$z(t_2) = \mathbf{\Phi}(t_2, t_1)z(t_1) + \int_{t_1}^{t_2} \mathbf{\Phi}(t_2, \tau)[\mathbf{T}w(\tau) + \mathbf{U}v(\tau)]d\tau \tag{14}$$

where $\mathbf{\Phi}$ is the transition matrix of $\mathbf{H}$. Defining the augmented state covariance matrix by $\mathbf{\Omega} = \mathbb{E}\left[z(t)z^T(t)\right]$ the autocorrelation of z is given by

$$\mathbb{E}\left[z(t_2)z^T(t_1)\right] = \begin{bmatrix} \mathbb{E}\left[x(t_2)x^T(t_1)\right] & \mathbb{E}\left[x(t_2)\tilde{x}^T(t_1)\right] \\ \mathbb{E}\left[\tilde{x}(t_2)x^T(t_1)\right] & \mathbb{E}\left[\tilde{x}(t_2)\tilde{x}^T(t_1)\right] \end{bmatrix} = \mathbf{\Phi}(t_2, t_1)\mathbb{E}\left[z(t_1)z^T(t_1)\right] = \mathbf{\Phi}(t_2, t_1)\mathbf{\Omega} \tag{15}$$

From Eq. (15) the first term in Eq. (9) can be readily obtained by writing the product in partitioned form. Similarly, to compute the second term in Eq. (9) the cross-correlation of z and v can be computed from the product

$$\mathbb{E}\left[z(t_2)v^T(t_1)\right] = \begin{bmatrix} \mathbb{E}\left[x(t_2)v^T(t_1)\right] \\ \mathbb{E}\left[\tilde{x}(t_2)v^T(t_1)\right] \end{bmatrix} = \mathbf{\Phi}(t_2, t_1)\mathbf{UR} \tag{16}$$

The previous equations allow to find the residual correlations when the Kalman filter is operating under sub-optimal conditions (environmental changes, damage, changing input statistics, etc.). Under ideal conditions and stationarity the Kalman gain is $\mathbf{K} = \mathbf{PC}^T\mathbf{R}^{-1}$, and the residual is a white process with Eq. 9 reducing to [27]

$$\mathcal{R}_{ee}(t_2, t_1) = \mathbf{R}\delta(t_2 - t_1) \tag{17}$$

2.3. Frequency domain analysis

The frequency domain version of Eq. (9) is now developed. For this purpose the power spectral density (PSD) of the residual, $\mathbf{S}_{ee}$, is found formally by first combining the Laplace transform of Eqs. (3) and (5), resulting in

$$E(s) = \left[\mathbf{I} + \mathbf{C}(s\mathbf{I} - \mathbf{A})^{-1}\mathbf{K}\right]^{-1} Y(s) = \mathbf{T}_1(s)Y(s) \tag{18}$$

where E and Y denote, respectively, the Laplace transform of e and y, and

$$\mathbf{T}_1(s) = \left[\mathbf{I} + \mathbf{C}(s\mathbf{I} - \mathbf{A})^{-1}\mathbf{K}\right]^{-1} \tag{19}$$

Similarly, combining the Laplace transform of Eq. 1 (with $\bar{\mathbf{A}}$ replacing $\mathbf{A}$) and Eq. 2 results in

$$Y(s) = \mathbf{C}\left[s\mathbf{I} - \bar{\mathbf{A}}\right]^{-1}\mathbf{B}W(s) + V(s) = \mathbf{T}_2(s)W(s) + V(s) \tag{20}$$

where W and V denote, respectively, the Laplace transform of w and v, and

$$\mathbf{T}_2(s) = \mathbf{C}\left[s\mathbf{I} - \bar{\mathbf{A}}\right]^{-1}\mathbf{B} \tag{21}$$

The innnovations PSD is formally obtained by combining the last two equations (evaluated at $s = i\omega$) and taking expectation [32]

$$\mathbf{S}_{ee}(\omega) = 2\pi\mathbf{T}_1(\omega)\mathbf{T}_2(\omega)\mathbf{Q}\mathbf{T}_2^*(\omega)\mathbf{T}_1^*(\omega) + 2\pi\mathbf{T}_1(\omega)\mathbf{R}\mathbf{T}_1^*(\omega) \tag{22}$$

where * denotes the Hermitian transpose. For stationary processes the correlation function of the residual is related to the PSD by the Wiener-Khinchin theorem

$$\mathcal{R}_{ee}(\tau) = \int_{-\infty}^{\infty} \mathbf{S}_{ee}(\omega)e^{i\omega\tau}d\omega \tag{23}$$

where $\tau = t_2 - t_1$. Under optimal operating conditions the Kalman gain is given by $\mathbf{K} = \mathbf{P}\mathbf{C}^T\mathbf{R}^{-1}$ and the PSD of the residual is

$$\mathbf{S}_{ee}(\omega) = 2\pi\mathbf{R} \quad \omega \in (-\infty, \infty) \tag{24}$$

2.4. Effect of structural damage in $\mathbf{S}_{ee}$

The effect of structural damage in $\mathbf{S}_{ee}$ has been studied elsewhere, and thus only a summary of the main result is discussed herein. Writing $\mathbf{T}_2$ in terms of the spectral decomposition of $\left[s\mathbf{I} - \bar{\mathbf{A}}\right]^{-1}$

$$\mathbf{T}_2(s) = \mathbf{C}\mathbf{\Phi}\mathbf{\Lambda}(s)\mathbf{\Phi}^{-1}\mathbf{B} \tag{25}$$

it was shown that the product $\mathbf{T}_1(p_j)\mathbf{T}_2(p_j)$ evaluated at a pole p_j of the open-loop system is bounded, and that structural damage induces peaks in $\mathbf{S}_{ee}$ at frequencies close to the affected vibration frequencies [30]. The appearance of peaks in the residual spectral density results from the violation of the following orthogonality condition that holds when the structure is undamaged

$$\mathbf{T}_1(p_j)\mathbf{C}\phi_j = 0 \tag{26}$$

where ϕ_j is the eigenvector corresponding to p_j [30]. Thus, when the structure is in a healthy condition the eigenvectors at the sensors are orthogonal to the transfer function $\mathbf{T}_1$ evaluated at the corresponding pole. The appearance of peaks in the residual spectral density is equivalent to the appearance of peaks in the frequency domain output of modal filters developed based on spatial filtering [33]. In spatial filtering the response measurements are combined such that the output of the combiner law is orthogonal to all modes on a pre-defined bandwidth; under these conditions structural damage induces peaks in the calibrated filter frequency response function. The Kalman filter can thus be interpreted as a modal filter calibrated to achieve a residual with a constant spectral density when the structure is in a healthy state.

2.5. Effect of temperature field variations in $\mathbf{S}_{ee}$

Smooth variations in the temperature field of a structure induce global changes in the stiffness matrix that can be approximately modeled as $\Delta\mathbf{K}_s = \alpha(T)\mathbf{K}_s$, were $\alpha(T)$ is a constant associated with the temperature-material behavior and $\mathbf{K}_s$ is the structure stiffness matrix. As a result, the eigenvectors of the system under smooth variations of the temperature field are approximately a scaled version of the eigenvectors of the undamaged system

$$\tilde{\phi}_j \approx \beta(T)\phi_j \tag{27}$$

where $\beta(T)$ is a temperature-dependent scaling factor. It is worth to point out that the previous relation has been experimentally verified in large-scale structures under different environmental conditions [34,15]. The previous result implies that the orthogonality condition in Eq. (26) becomes

$$\mathbf{T}_1(p_j)\mathbf{C}\tilde{\phi}_j \approx \beta(T)\mathbf{T}_1(p_j)\mathbf{C}\phi_j = 0 \tag{28}$$

It can be concluded that under smooth variations of the temperature field the orthogonality condition is satisfied, and thus the residual spectral density $\mathbf{S}_{ee}$ remains approximately constant, with the same value of the spectral density of the undamaged structure. The two properties given by Eqs. (26) and (28) form the basis of the approach proposed herein to decouple temperature effects from structural damage. It is worth to point out that an equivalent property is also seen in spatial filters, where environmental effects cause a shift in the filter frequency response function, without the appearance of new peaks [33].

3. Damage-sensitive features: whiteness and damage measures

Structural damage induces a correlation in the Kalman filter residual process while the residual remains uncorrelated under smooth variations in the temperature field, as discussed in the previous section. In order to assess if a finite-length realization of the residual process is correlated (for damage detection) a whiteness statistic is proposed. The whiteness statistic is complemented by a damage index defined as a peakness measure for damage quantification purposes. The damage index is such that it attains a value of zero when the structure is undamaged, and approaches one asymptotically as damage increases.

3.1. Whiteness deviation measure

In practical applications the correlation function and the power spectral density are estimated from finite length time-histories. Thus, an statistical test needs to be performed to assess if a given sequence qualifies as a white process in terms of statistical significance. Assessing the whiteness of a sequence can be reduced to a model assessment problem. In this context the task is to check if a white residual process model is consistent with the data. A Bayesian whiteness test is proposed to perform this task [35]. The approach consists in drawing simulated values from the posterior predictive distribution and comparing them to the observations (vibration data).

For this purpose a test statistic is defined to measure the discrepancy between the model and the data. The test statistic proposed to measure the whiteness of the residual sequence is

$$WT(e) = \textit{number of switches in the sign of } e \tag{29}$$

Intuitively, if the residual is white the statistic WT has a large value due to the (erratic) nature of the residual, whereas WT decreases as the residual correlation increases since the time-history becomes smoother. The value of the statistic is compared to a Bayesian p-value (tail-area probability), defined as the probability that the simulated data could be more extreme than the observed data

$$p = P(WT(e) \geqslant WT(\bar{e})|\mathbf{Y}) \tag{30}$$

where P denotes a probability measure, $\bar{e}$ is the simulated or predicted sequence of the residual for the undamaged structure, and $\mathbf{Y}$ is the measured vibration data. The statistic WT is a random variable, since it is a function of the random process e. It is expected that the accuracy of the test increases as the length of the vibration data time history considered increases, i.e., the probability of correctly estimating the state of structural integrity increases asymptotically to one as the measurements length increases to infinity. As will be seen in the numerical results section, the probability becomes close to one for time histories of length considered in practice, and thus the asymptotic result is useful for applications.

The Bayesian whiteness test is suitable when the number of observations is not enough to resort to asymptotic classical statistics. Under certain conditions the Bayesian and classical results are equivalent in the limit of increasing observations [35]. Other measures of whiteness previously proposed in the literature can also be adopted and incorporated to provide a more comprehensive set of test measures. These whiteness measures include, but are not limited to, the irregularity factor, crossing rates and bandwidth measures [29,30,32].

3.2. Damage measure

The second feature for damage evaluation is a peak indicator (or peak statistic) which tests for the presence of peaks in a given frequency bandwidth. Interpreting the power spectral density as a scaled version of a probability density function, the truncated spectral moments (for each frequency bandwidth) are defined by

$$\lambda_j = \int_{\omega_1}^{\omega_2} \xi^j \mathbf{S}_{e_i e_i}(\xi) d\xi \tag{31}$$

The following normalized damage index is proposed as a quantitative measure of damage

$$D = 1 - \sqrt{3}\frac{\omega_2 + \omega_1}{\omega_2 - \omega_1}\frac{\left[\lambda_2/\lambda_0 - (\lambda_1/\lambda_0)^2\right]^{1/2}}{\lambda_1/\lambda_0} \tag{32}$$

The second term in Eq. (32) is the scaled coefficient of variation of the spectral density normalized in the range $[\omega_1, \omega_2]$. The scaling is such that when the system is healthy (constant spectral density or uniform distribution) the index value is $D = 0$, whereas the index approaches $D \to 1$ as damage increases (the spectral density approaches a Dirac delta function). The proposed index has the advantage that it is normalized to the interval $[0, 1]$.

4. Summary of the proposed approach

The proposed approach for damage identification under changing environmental conditions is summarized as follows.

1. From measured data at a reference healthy state extract the matrices $\{\mathbf{A}_d(T), \mathbf{C}_d(T), \mathbf{K}_d(T)\}$ for different environmental conditions.
2. Compute the innovations using the discrete version of Eqs. (3) and (4).
3. Compute the correlation and spectral density of the innovations to verify the expected behavior under healthy conditions.
4. When data of a potentially damaged structure is available compute the innovations correlations using the identified matrices at the interrogation tempearture.
5. Compute *WT* defined in Eq. (29), the spectral moments defined by Eq. (31) and the damage index defined by Eq. (32).
6. For damage detection and quantification use the damage index *D* and compare *WT* from interrogation data to the cut-off value obtained from the reference healthy data.

5. Numerical verification

In this section we present numerical results aimed at studying the effectiveness of the proposed damage estimation approach for structural systems subjected to changing temperature fields. We begin by discussing the causal effects of temperature field variations in structural systems, which will be used to define temperature-dependent models for structural behavior.

5.1. Physical effects of temperature field variations in structures

A variation in the temperature field in the surroundings of a structural system induces physical changes that alter its vibration characteristics. In typical applications the two main physical changes induced in the structure are:

1. Changes in mechanical properties of the materials
2. Changes in boundary conditions

Changes in material properties and boundary conditions are the main causes of the variability in the vibration characteristics (frequencies, mode shapes and damping) observed in structures under varying environmental conditions.

5.1.1. Temperature effect in mechanical properties of materials

It is well-known that temperature variations affect the microscopic and macroscopic properties of most materials. For example, structural steel subjected to high temperatures experiences a decrease in the effective elastic modulus and an increase in ductility, while at low temperatures the converse occurs. Several models have been proposed to describe the temperature-elastic modulus relationship of structural steel. The following recently proposed model will be adopted herein [36]

$$E(T) = e_0 + e_1 T + e_2 T^2 + e_3 T^3 \quad T \geqslant 0\,^{\circ}\mathrm{C} \tag{33}$$

where the temperature T is given in Celsius degrees and

$$e_0 = 206\ \mathrm{GPa}$$
$$e_1 = -4.326 \times 10^{-2}\ \mathrm{GPa}/^{\circ}\mathrm{C}$$
$$e_2 = -3.502 \times 10^{-5}\ \mathrm{GPa}/(^{\circ}\mathrm{C})^2$$
$$e_3 = -6.592 \times 10^{-8}\ \mathrm{GPa}/(^{\circ}\mathrm{C})^3$$

For temperatures below $0^{\circ}C$ the relationship is approximately linear with slope e_1 (ASME B31.1–1995). The model is depicted in the left panel of Fig. 1, where it can be observed that for temperatures up to about 200°F the relationship is approximately linear. It should be pointed out that the relationship between vibration frequencies of structures and the elastic modulus is nonlinear, and approximately of the form $f \sim \sqrt{E}$. To model the temperature-dependent behavior of reinforced concrete the following recently proposed model will be adopted [37]

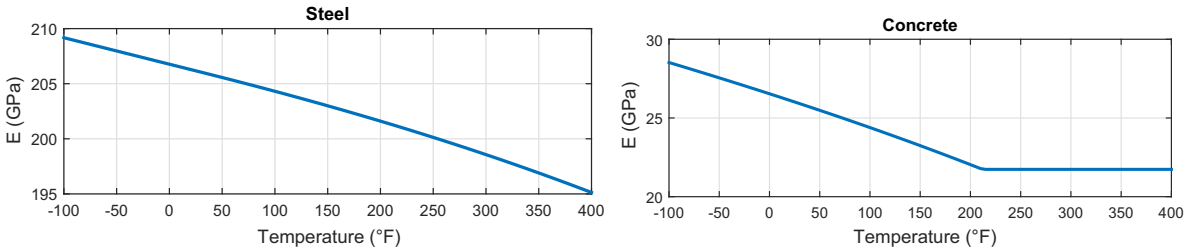

Fig. 1. Temperature-elastic modulus relationship for A36 structural steel and 4 ksi concrete.

$$f'_{c,T} = \begin{cases} f'_c[1.0 - 0.003125(T-20)] & T < 100\,^{\circ}\mathrm{C} \\ 0.75 f'_c & 100\,^{\circ}\mathrm{C} \leqslant T \leqslant 400\,^{\circ}\mathrm{C} \\ f'_c[1.33 - 0.00145T] & 400\,^{\circ}\mathrm{C} < T \end{cases} \tag{34}$$

where f'_c is the 28 day compressive strength at 20 °C and T is the temperature in °C. The concrete compressive strength can be related to its elastic modulus using the following expression [38]

$$E_c = 1820\sqrt{f'_c} \tag{35}$$

where f'_c is in ksi. The model is illustrated in the right panel of Fig. 1. The temperature model will be adopted to generate the synthetic data for the numerical validation studies to be carried out in following sections; the model is not used to implement the proposed damage detection approach.

5.1.2. Temperature effect in boundary conditions

Variations in the environment surrounding a structure induce changes in the boundary conditions that can potentially have an important impact in its vibration characteristics [39]. It has been shown using field experiments in bridges that temperature variations induce expansions and contractions of bridge decks [40,41]. These movements affect the expansion joints inducing temporal changes in the boundary conditions. In Ref. [7] the effect of freezing of the supports was studied in a typical highway bridge. The effect of damage and changing environment was considered by introducing a cut in the bottom flange of the main girders. It was shown that the frequencies of the damaged bridge at freezing temperatures are larger (by a factor of $1.5-2$) than the frequencies of the undamaged bridge at normal temperatures. It was concluded that the probable cause of the difference was a change in the abutment boundary conditions caused by freezing of accumulated moisture.

5.2. System description

The system considered is the continuous steel beam model depicted in Fig. 2; the model is consistent with steel girder bridges typically used in highway overpasses [42]. The beam is subjected to a uniform temperature field T along its length and depth, with the temperature-elastic modulus relationship modeled using Eq. (33). The damage measures previously discussed are employed to detect and quantify damage; their uncertainty and robustness under different operating conditions is studied, and conclusions regarding their accuracy and applicability are drawn.

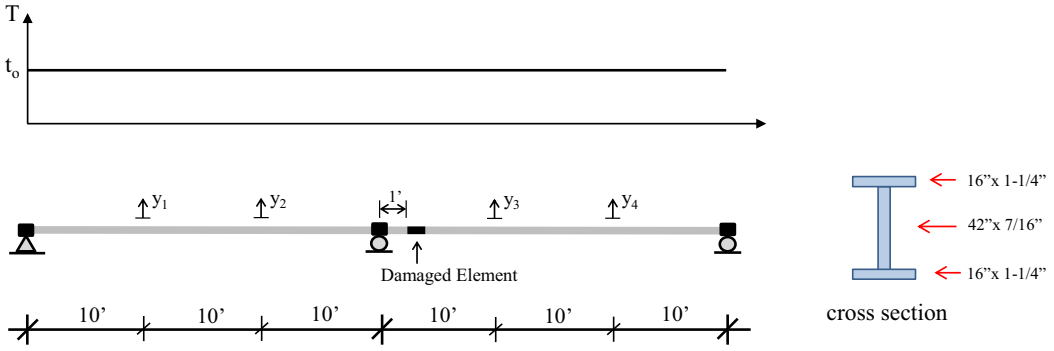

Fig. 2. Continuous beam model subjected to a uniform temperature field. The damage scenario is considered as a 15% reduction in stiffness of a 2 ft wide element located 1 ft away from the middle support.

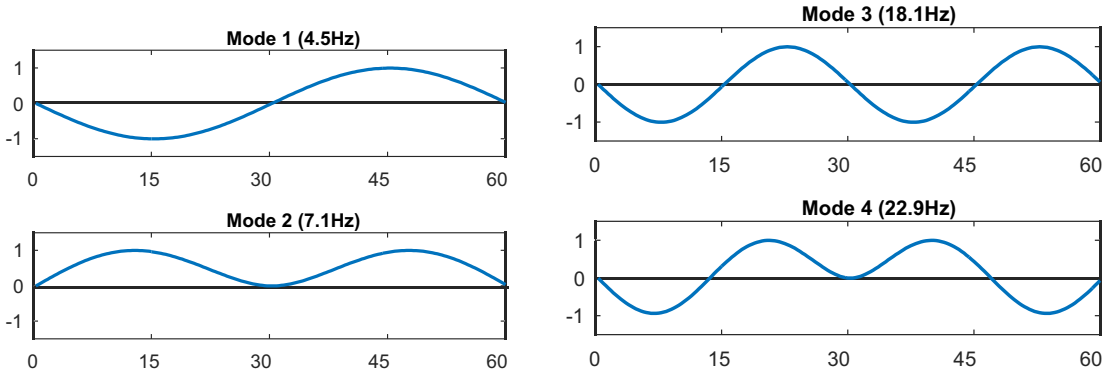

Fig. 3. Modes of vibration at the reference temperature $T_R = 70^{\circ}$.

The continuous beam was modeled using a finite element formulation. For this purpose the beam was divided in 60 elements of 1 foot of length; the number of elements was selected based on a convergence analysis of the dynamic properties as the number of elements was increased. For the beam section a mass density $\rho = 7.37 \times 10^{-7}\, kip - s^2/in/in^3$ was used. The section properties were computed using the cross section depicted in Fig. 2. Modal damping with a damping ratio of 5% in all modes was considered.

The mechanical properties of materials, and hence the dynamic properties of the beam are temperature-dependent, as discussed in previous sections. For this reason a reference temperature needs to be established for analysis purposes. The reference temperature for the results shown in this section is $T_R = 70^{\circ}$F. The first four modes of vibration based on the properties at the reference temperature are shown in Fig. 3. These modes are considered to be the modes of the undamaged system at the reference temperature, and as discussed before, the shape of the modes is not greatly affected by smooth changes in the temperature field.

A sensitivity analysis of the vibration frequencies due to temperature variations and damage was performed to define the temperature resolution. Fig. 4 shows the temperature-frequency relationship for the first four modes of vibration; as the

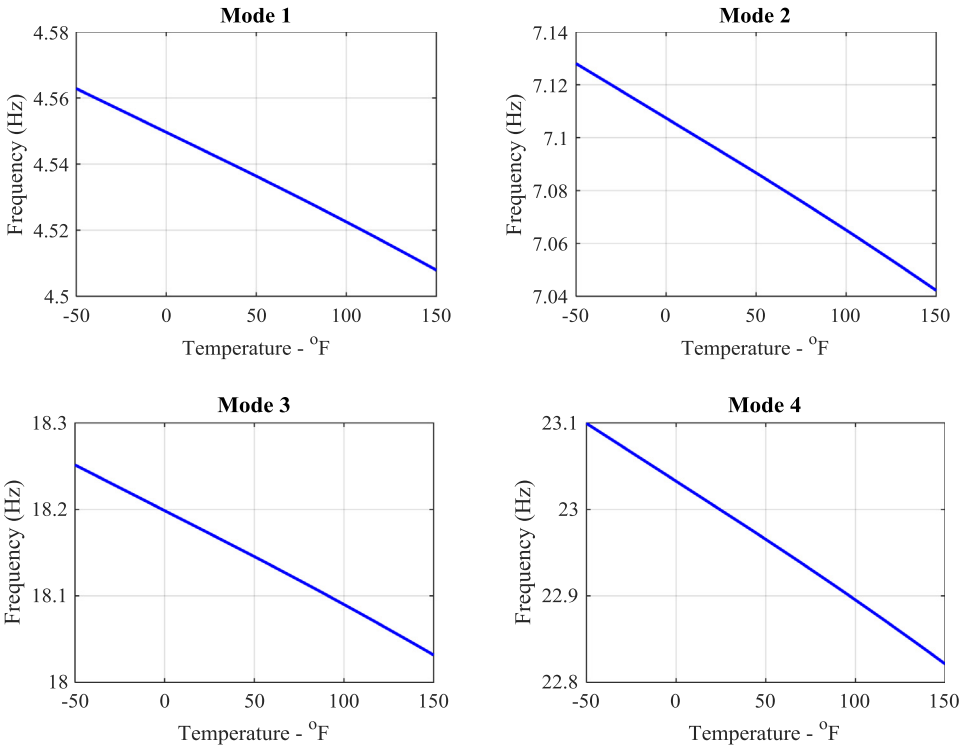

Fig. 4. Variation of the vibration frequencies caused by changes in the uniform temperature field.

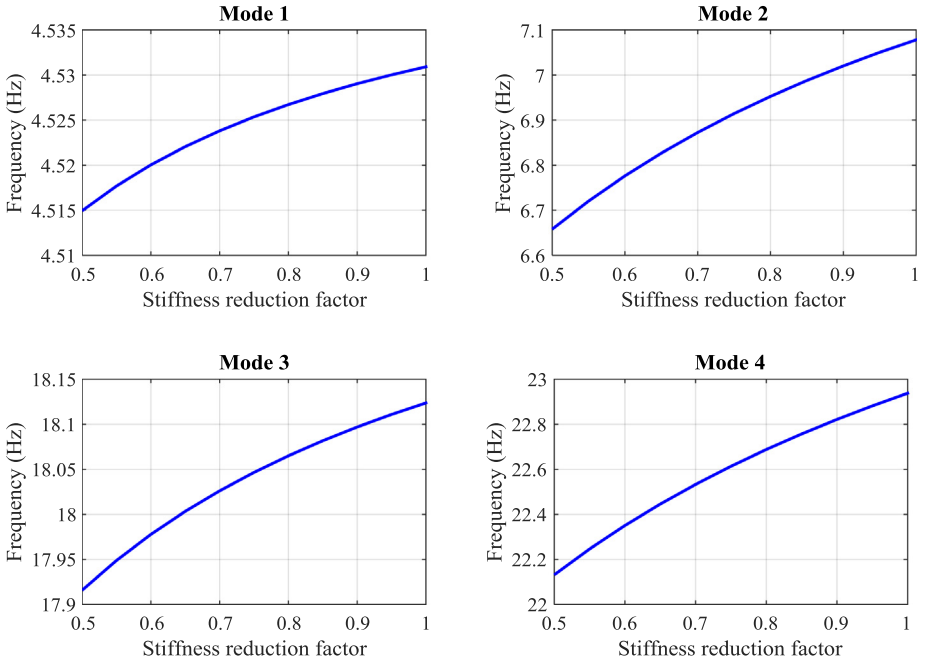

Fig. 5. Variations of the vibration frequencies caused by damage; Damage is defined as a reduction in stiffness of a 2 ft wide element located 1 ft away from the middle support (See Fig. 2).

temperature increases the elastic modulus (and the stiffness) decreases, and thus the vibration frequencies decay. The relationship is slightly nonlinear at high temperatures, but approximately linear in the range $(-50, 100)$, which is of interest in many structural engineering applications.

Structural damage will be modeled by applying a scaling factor to the flexural stiffness of a 2 ft wide element near the middle support (see Fig. 2); the factor is used to model physical damage such as severe cracking, delamination and loss of cross section due to corrosion. Fig. 5 depicts the damage-frequency relationship as a function of the scaling factor. As expected, modes 1 and 3 are almost unaffected, since the curvature of these modes is small in the damaged region. When considered together, Figs. 4 and 5 provide the frequency sensitivity relations for damage and a uniform temperature field for the beam in Fig. 2.

5.3. Effect of temperature field variations and damage in the Kalman filter residual

The effect of temperature field variations and structural damage in the Kalman filter residual is studied next. The output consists of velocity measurements at locations $\{y_1, y_2, y_3, y_4\}$ depicted in Fig. 2. The measurement noise and forcing input spectral density were selected as identity matrices of proper dimensions. The residual spectral density at the sensor y_2 for the undamaged beam at the reference temperature, and at the interrogation temperature $T_I = 20^{\circ}\text{F}$ are shown in Fig. 6. The spectral densities depicted in Fig. 6 are based on the direct computation of the transfer functions $\mathbf{T}_1(s)$ and $\mathbf{T}_2(s)$ defined, respectively, by Eqs. (19) and (21). The interrogation temperature used is assumed to be the average air temperature at the structure location, assumed to be known. As expected, based on the analysis in previous sections, the residual

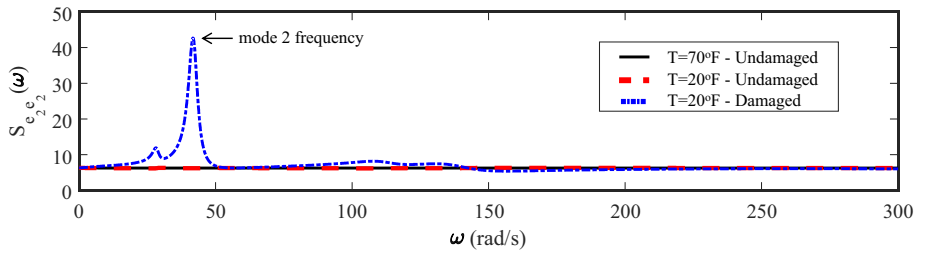

Fig. 6. Residual spectral density at measurement y_2 location for the reference temperature field, the interrogation temperature field with no damage, and the interrogation temperature field with damage.

spectral density remains constant and almost insensitive to the temperature change. This is because the orthogonality condition in Eq. (26) is satisfied when the undamaged structure is subjected to smooth variations in the temperature field as discussed before. Similar results were obtained for variations of the temperature field in the range $(-50, 150)$.

To consider the effect of structural damage the scaling factor was selected as 0.85, i.e., a 15% reduction in flexural stiffness was applied to the element labeled as "damaged element" in Fig. 2, at the interrogation temperature $T_I = 20°\text{F}$. The PSD of the residual e_2 for the damaged beam is shown in Fig. 6, where a peak is seen to appear close to the second mode vibration frequency. The second mode is the lowest affected mode with significant participation in the response. Similar results were obtained for different combinations of the reference and interrogation temperature fields in the range $(-50, 150)$, and for different stiffness reduction factors between 10% and 50%; the results presented herein are representative of the considered range.

The previous results show that the residual spectral density remains constant under temperature field variations, while peaks arise in a subset of the vibration frequencies in the presence of damage. This is the main feature of the proposed approach to decouple temperature variations and structural damage. As mentioned before the previous results are based on the direct computation of the transfer functions $\mathbf{T}_1(s)$ and $\mathbf{T}_2(s)$. In practice these functions are not available and the residual spectral density needs to be estimated from the response measurements as discussed in the following section.

5.4. Application using synthetic measured data

Although the previous results are encouraging and serve to validate the premises of the approach under ideal conditions, for practical applications the transfer functions $\mathbf{T}_1$ and $\mathbf{T}_2$ are not available in general. Under these conditions the residual spectral density needs to be estimated from finite-length time histories. A realization of the input/output processes of length 5 min with a sampling frequency of $100Hz$ was generated, and used to estimate the Kalman filter residual correlation function $\mathcal{R}_{ee}$ and residual PSD $\mathbf{S}_{ee}$ at the reference temperature (T_R) and interrogation temperature (T_I). The residual was computed using a similar procedure to that discussed in Ref. [30]; for this purpose the residual is estimated based on a realization of the filter matrices using output-only system identification [43]. It should be pointed out that although the identified system is not in physical coordinates the residual can be computed using Eq. (4).

The correlation function and PSD of e_2 are depicted in Fig. 7. As can be seen, for the healthy system the correlation function is highly peaked with value close to zero for $\tau > 0$ which consistent with a white noise process, while the PSD is approximately constant for both the reference and interrogation temperatures. The PSD was estimated using the Barlett method of periodograms [44].

The correlation function and spectral density for the damaged beam are also shown in Fig. 7, where it can be seen that the correlation function shows a deviation from zero for $\tau > 0$, which is indicative of correlation in the realization of the residual process. This is confirmed by the peak observed in the PSD at a frequency close to the vibration frequency of the second mode in the lower panel of Fig. 7. The results confirm that the residual PSD is almost insensitive to temperature variations, while it is greatly affected by damage, which is the main feature of the approach presented herein. In order to obtain quantitative estimates of the degree of damage the damage-sensitive measures discussed in Section 3 are employed. These measures are needed for automated (unsupervised) structural health monitoring, since it would be unpractical to examine the residuals correlation and PSD manually.

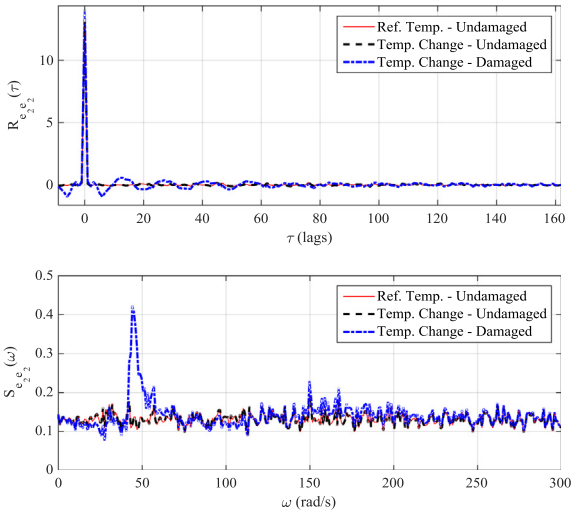

Fig. 7. Upper panel: Correlation function of the residual at location of measurement y_2. Lower panel: Power spectral density of the residual at location of measurement y_2.

5.5. Damage measures large-sample behavior

In this section we study the large-sample behavior of the statistics used for damage detection and quantification to find the probability of correctly detecting damage for a given measurement sequence.

The probability density function (PDF) of $WT(\bar{e})$ for the undamaged and damaged system are depicted on the left panel of Fig. 8 for a 5 min measurement history based on a Monte Carlo analysis, i.e., based on computing WT for $100,000$ random sequences of the measurement data under both undamaged and damaged conditions. The cutoff value (vertical dashed line) for a significance level $p = 0.05$ is $WT_p = 4875$. This value serves as a benchmark to determine if a residual sequence corresponds to a healthy or damaged structure. The overlap of the two PDF means that some damaged sequences might be wrongly classified as undamaged, in which case the statistical test gives a false-negative damage estimate. However, the probability of a false-negative is directly related to the length of the time history considered, and thus can be reduced by increasing the measurement record as discussed next.

The random variable $WT_U - WT_D$ where subscripts U and D stand for, respectively, the undamaged and damaged states, is shown in the right panel of Fig. 8. This variable provides a useful way to approximately assess the accuracy of the statistical test. The overlap region corresponds to the region where $WT_U - WT_D < 0$. The overlap of two PDF decreases as the length of the time history considered increases, with an increase in the index τ. This feature allows to reduce the probability of a false-negative by increasing the probability of a correct detection. As before this result is based on a Monte Carlo analysis.

The accuracy of the test, i.e., the probability of correctly detecting damage will now be assessed. It is expected that this probability should increase monotonically to one as the length of the data time history increases; in essence, the uncertainty in the statistical test decreases as the amount of information increases. The probability of detecting damage correctly was computed for different length of the data time history, and is shown in Fig. 9; the probabilities where computed using a Monte Carlo analysis. As expected the probability approaches one monotonically as the length of the measurements increase. This is a powerful feature of the proposed approach, since any desired accuracy can be achieved by selecting an appropriate time interval for analysis. The second damage-sensitive feature is the damage index in Eq. (32). This damage index is a measure of the peak in the PSD, and approaches one as the PSD approaches a Dirac delta in a considered range. The damage index D for the 20% stiffness reduction discussed above was found to be $D = 0.23$.

The sensitivity of the approach to errors in the definition of the measurement noise covariance matrix $\mathbf{R}$ and the input process covariance matrix $\mathbf{Q}$ was assessed numerically. It was found that the method is reliable for errors up to 30% in

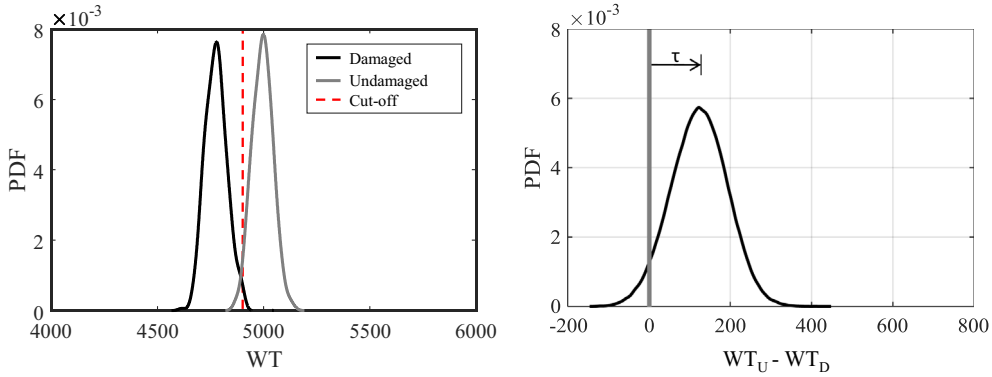

Fig. 8. Left panel: Random variable WT for the damaged and undamaged beam for a measurement record of 5 min and 20% damage. Right panel: Random variable $WT_U - WT_D$, where WT_U and WT_D are, respectively, the statistic WT of the undamaged and damaged structure.

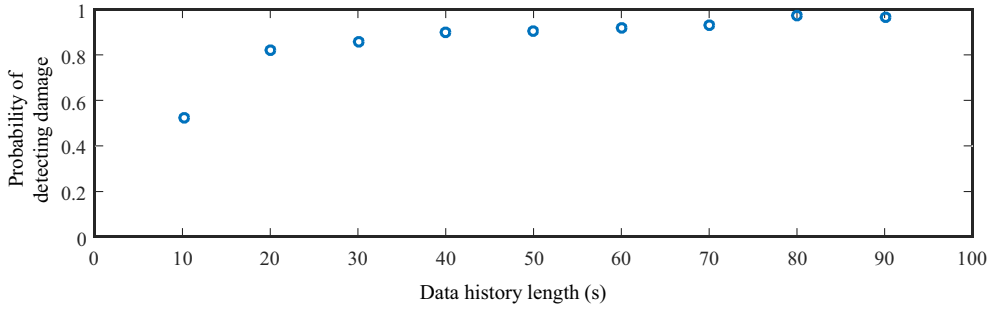

Fig. 9. Assessment of the accuracy of the test (probability of detecting damage correctly) as a function of the data record length. The accuracy of the test increases monotonically as the record length increases.

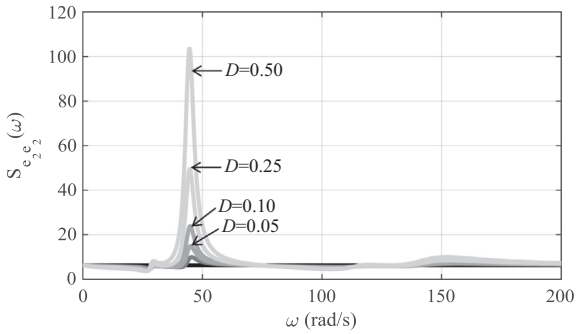

Fig. 10. Effect of damage in the residual spectral density; as damage increases the spectral density approaches a Dirac delta in the main affected frequencies, while the proposed damage index approaches one.

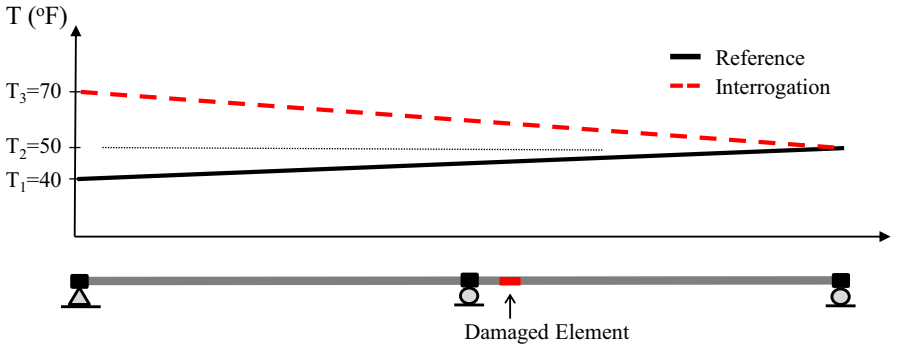

Fig. 11. Non-uniform reference and interrogation temperature fields.

the definition of the matrices. For errors greater than 30% the correlations in the residual due to the errors in **Q** and **R** cannot be distinguished from the correlation caused by damage, since as shown in Ref. [30] errors in these matrices also induce a correlation in the residual. In future work the approach will be extended to account for both types of correlations according to their decay rate.

Finally, the spectral density of the residual computed for increasing damage factors between 0 and 0.9 is shown in Fig. 10. As can be seen, as damage increases the spectral density approaches a Dirac delta, as expected, in which case the damage index D approaches one.

5.6. Robustness under non-uniform temperature fields

Under typical environmental conditions the temperature field is not uniform, but instead varies slowly throughout the structure in space and time. An scenario where the temperature field varies linearly over the length of the beam is now considered. The reference and interrogation temperature fields are depicted in Fig. 11. The temperature fields are consistent with fields measured using thermocouples in instrumented overpass bridges throughout a 24-h period [9,20]. The rest of the parameters will remain as before.

The residual PSD at sensor y_2 for the undamaged beam at the reference temperature field, the interrogation temperature field with no damage, and the interrogation temperature field with damage are shown in Fig. 12. As can be seen the PSD remains approximately constant for the reference field and the interrogation field when the beam is undamaged, while it

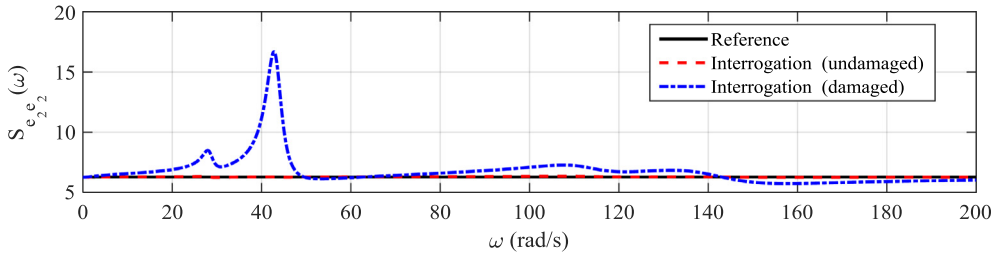

Fig. 12. Residual spectral density at measurement y_2 location for the reference field, the interrogation field with no damage, and the interrogation temperature field with damage for the non-uniform fields depicted in Fig. 11.

shows a peak for the damaged beam. This result shows that the proposed framework is robust in the presence of smooth non-uniform temperature fields typically observed in structures.

6. Conclusion

In this paper a Kalman filtering based framework for structural health monitoring under changing environmental conditions was presented. The proposed approach is based on the well-known property that the Kalman filter residual is a realization of a white process when the filter is operating under optimal conditions. To decouple environmental effects and structural damage the following additional properties of the residual power spectral density were employed: i) local changes in the structure caused by structural damage induce peaks in the residual spectral density; ii) under global changes caused by environmental variations the residual spectral density remains approximately constant.

In the proposed approach the residual spectral density is estimated from a finite length realization of the residual process, which in turn is estimated from vibration response measurements obtained using an array of sensors deployed at limited spatial locations throughout the structure. To assess if a finite length realization of the residual process statistically qualifies as a white process a correlation (whiteness) Bayesian test was proposed for damage detection. The test was complemented with a damage index in the form of a peak indicator that allows to obtain a measure of the degree of damage (damage quantification). The proposed damage index is normalized such that it attains a value of zero when the structure is undamaged, and asymptotically approaches one as damage increases.

The proposed approach was numerically verified in a continuous beam model of a bridge under uniform and non-uniform temperature fields. It was shown that the approach has the capability to decouple changes induced by structural damage and normal fluctuations of the temperature field, providing a damage index as a quantitative measure of damage for structural health monitoring applications. In future work the approach will be validated using laboratory experiments and field measurements from instrumented structures. In this setting the effect of environmental variations in the boundary conditions will also be assessed.

References

[1] S. Doebling, C. Farrar, M. Prime, A summary review of vibration-based damage detection and system identification methods, Shock Vib. Dig. 30 (2) (1998) 91–105.
[2] S. Nagarajaiah, K. Erazo, Structural monitoring and identification of civil infrastructure in the United States, Struct. Monit. Maintenance Int. J. 3 (1) (2016).
[3] K. Erazo, E. Hernandez, Bayesian model-data fusion for mechanistic postearthquake assessment of building structures, J. Eng. Mech. (2016), https://doi.org/10.1061/(ASCE)EM.1943-7889.0001114(04016062).
[4] K. Worden, G. Manson, The application of machine learning to structural health monitoring, Proc. R. Soc. A 365 (2006) 515–537.
[5] K. Erazo, E. Hernandez, Uncertainty quantification of state estimation in nonlinear structural systems with application to seismic response in buildings, ASCE-ASME J. Risk Uncertainty Eng. Syst. Part A Civ. Eng. (2016), https://doi.org/10.1061/AJRUA6.0000837, B5015001.
[6] Y. Park, A. Ang, Y. Wen, Seismic damage analysis of reinforced concrete buildings, J. Struct. Eng. 111 (4) (1985) 740–757.
[7] S. Alampalli, Influence of in-service environment on modal parameters, in: Proceedings of the XVI International Modal Analysis Conference, 1998, pp. 111–116.
[8] C. Farrar, S. Doebling, P. Cornwell, E. Straser, Variability of modal parameters measured on the Alamosa Canyon Bridge, in: Proceedings of the XV International Modal Analysis Conference, 1997, pp. 257–263.
[9] S. Sohn, M. Dzonczyk, E. Straser, A. Kiremidjian, K. Law, T. Meng, An experimental study of temperature effect on modal parameters of the Alamosa Canyon Bridge, Earthquake Eng. Struct. Dynam. 28 (1999) 879–897.
[10] Farrar, et al., Dynamic characterization and damage detection in the I-40 bridge over the Rio Grande, Los Alamos National Laboratory Report: LA-12767-MS, 1994.
[11] E.J. Cross, G. Manson, K. Worden, G. Pierce, Features for damage detection with insensitivity to environmental and operational variations, Proc. R. Soc. A 468 (2012) 4098–4122.
[12] H. Li, S. Li, J. Ou, H. Li, Modal identification of bridges under varying environmental conditions: temperature and wind effects, Struct. Control Health Monit. 17 (2010) 495–512.
[13] L. Sun, Z. Min, Temperature effects on modal parameters and its experimental validation, in: SPIE Smart Structures and Materials Nondestructive Evaluation and Health Monitoring, 2010, pp. 76502–76502L.
[14] T.-Y. Hsu, C.-H. Loh, Damage detection accommodating nonlinear environmental effects by nonlinear principal component analysis, Struct. Control Health Monit. 17 (2010) 338–354.
[15] Y. Xia, B. Chen, S. Weng, Y. Ni, Y. Xu, Temperature effect on vibration properties of civil structures: a literature review and case studies, J. Civil Struct. Health Monit. 2 (2012) 29–46.
[16] M.M. Wahab, G. De Roeck, Damage detection in bridges using modal curvatures: application to a real damage scenario, J. Sound Vib. 226 (2) (1999) 217–235.
[17] A.-M. Yan, G. Kerschen, P. De Boe, J.-C. Golinval, Structural damage diagnosis under varying environmental conditions-part i: a linear analysis, Mech. Syst. Signal Process. 19 (2005) 847–864.
[18] Kullaa, Elimination of environmental influences from damage-sensitive features in a structural health monitoring system, in: Structural Health Monitoring: Demands and Challenges, CRC Press, Boca Raton, Fl., 2001, pp. 742–749.
[19] B. Peeters, G. De Roeck, One-year monitoring of the Z24-bridge: environmental effects versus damage events, Earthquake Eng. Struct. Dynam. 30 (2001) 149–171.
[20] B. Moaveni, I. Behmanesh, Effects of changing ambient temperature on finite element model updating of the Dowling Hall footbridge, Eng. Struct. (2012) 58–68.
[21] C.R. Fritzen, G. Mengelkamp, A. Guemes, Elimination of temperature effects on damage detection within a smart structure concept, in: Proc. 4th Int. Workshop on Structural Health Monitoring, Stanford, CA., 2003, pp. 1530–1538
[22] A. Deraemaeker, E. Reynders, G. De Roeck, J. Kullaa, Vibration-based structural health monitoring using output-only measurements under changing environment, Mech. Syst. Signal Process. 22 (2008) 34–56.
[23] A.-M. Yan, G. Kerschen, P. De Boe, J.-C. Golinval, Structural damage diagnosis under varying environmental conditions-part ii: local PCA for non-linear cases, Mech. Syst. Signal Process. 19 (2005) 865–880.

[24] E. Reynders, G. Wursten, G. De Roeck, Output-only structural health monitoring in changing environmental conditions by means of nonlinear system identification, Struct. Health Monit. 13 (1) (2014) 82–93.
[25] R. Mehra, On the identification of variances and adaptive Kalman filtering, IEEE Trans. Autom. Control 15 (2) (1970) 175–184.
[26] R.E. Kalman, R.S. Bucy, New results in linear filtering and prediction theory, J. Basic Eng. (1961) 95–108.
[27] A. Gelb, Applied Optimal Estimation, The M.I.T. Press, Cambridge, 1996.
[28] P. Van Overschee, B. De Moor, Subspace Identification for Linear Systems, Kluwer Academic Publishers, 1996.
[29] R. Mehra, J. Peschon, An innovations approach to fault detection and diagnosis in dynamic systems, Automatica 7 (1971) 637–640.
[30] D. Bernal, Kalman filter damage detection in the presence of changing process and measurement noise, Mech. Syst. Signal Process. 39 (2013) 361–371.
[31] T. Kailath, An innovations approach to least-squares estimation, pt. I: linear filtering in additive white noise, IEEE Trans. Autom. Control 13 (1968) 646–655.
[32] L. Lutes, S. Sarkani, Random Vibrations: Analysis of Structural and Mechanical Systems, Elsevier, 2004.
[33] A. Deraemaeker, A. Preumont, Vibration based damage detection using large array sensors and spatial filters, Mech. Syst. Signal Process. 20 (2006) 1615–1630.
[34] W. Song, S. Dyke, Ambient vibration based modal identification of the Emerson bridge considering temperature effects, in: The 4th World Conference on Structural Control and Monitoring, 2006.
[35] A. Gelman, J. Carlin, H. Stern, D. Rubin, Bayesian Data Analysis, Chapman and Hall CRC, Boca Raton, Florida, USA, 2004.
[36] Luecke, et al., Mechanical properties of structural steels. NIST NCSTAR 1–3D Federal Building and Fire Safety Investigation of the World Trade Center Disaster, 2005.
[37] V. Kodur, Properties of concrete at elevated temperatures, ISRN Civil Eng. 1–15 (2014) 2014.
[38] American Association of State Highway and Transportation Officials, AASHTO LRFD Bridge Design Specifications, 1996.
[39] Sohn, Effects of environmental and operational variability on structural health monitoring, Philos. Trans. R. Soc. 28 (2007) 539–560.
[40] S. Moorty, C.W. Roeder, Temperature-dependent bridge movements, ASCE J. Struct. Eng. 118 (1992) 1090–1105.
[41] R.G. Rohrmann, M. Baessler, S. Said, W. Schmid, W.F. Ruecker, Structural causes of temperature affected modal data of civil structures obtained by long time monitoring, in: Proceedings of the XVII Int. Modal Analysis Conference, 1999, pp. 1–6.
[42] K. Barth, Steel bridge design handbook design Example 2a: two-span continuous straight composite steel I-girder bridge, Federal Highway Administration Report FHWA-IF-12-052 (2012) 21.
[43] D. Di Ruscio, Combined deterministic and stochastic system identification and realization: Dsr–a subspace approach based on observations, Model. Identification Control 17 (3) (1996) 193–230.
[44] J. Proakis, D. Manolakis, Digital Signal Processing, Prentice Hall, New Jersey, USA, 1996.